

Broken parity and a chiral ground state in the frustrated magnet CdCr₂O₄Gia-Wei Chern,¹ C. J. Fennie,² and O. Tchernyshyov¹¹*Department of Physics and Astronomy, Johns Hopkins University, Baltimore, Maryland 21218, USA*²*Department of Physics and Astronomy, Rutgers University, Piscataway, New Jersey 08854, USA*

(Received 13 June 2006; revised manuscript received 21 July 2006; published 30 August 2006)

We present a model describing the lattice distortion and incommensurate magnetic order in the spinel CdCr₂O₄, a good realization of the Heisenberg “pyrochlore” antiferromagnet. The magnetic frustration is relieved through the spin-Peierls distortion of the lattice involving a phonon doublet with odd parity. The distortion stabilizes a collinear magnetic order with the propagation wave vector $\mathbf{q}=2\pi(0,0,1)$. The lack of inversion symmetry makes the crystal structure chiral. The handedness is transferred to magnetic order by the relativistic spin-orbit coupling: the collinear state is twisted into a long spiral with the spins in the *ac* plane and \mathbf{q} shifted to $2\pi(0, \delta, 1)$.

DOI: [10.1103/PhysRevB.74.060405](https://doi.org/10.1103/PhysRevB.74.060405)

PACS number(s): 75.25.+z, 75.50.Ee

Frustration, defined as the presence of competing interactions, often leads to unusual effects in magnets, particularly when it is combined with a high symmetry.¹ A case in point is the antiferromagnet on the “pyrochlore” lattice that has a very high degeneracy of the ground state if magnetic interactions are restricted to nearest neighbors.² At the lowest temperatures such a magnet is expected to retain a finite entropy per unit volume, as was indeed observed in a group of pyrochlore magnets known as “spin ice.”³ It is also well known that frustrated magnets with a large degeneracy are prone to lattice distortions that reduce the frustration by lowering the symmetry.^{4,5} This effect was observed in antiferromagnetic spinel ZnCr₂O₄.^{6,7} Unfortunately, the distortion in this compound is rather intricate⁸: it involves at least four phonon modes with wave numbers $2\pi\{\frac{1}{2}, \frac{1}{2}, \frac{1}{2}\}$. Magnetic order in the distorted lattice is even more complex: the magnetic unit cell is said to contain as many as 64 spins.⁹ As a result, the basic story of a flexible pyrochlore¹⁰ does not apply to ZnCr₂O₄ and thus remains to be fully tested. Recent experimental characterization of another spinel CdCr₂O₄ by Chung *et al.*¹¹ presents us with an opportunity to do so.

Spinel ACr₂O₄ with various nonmagnetic ions on the A sites are nearly ideal $S=3/2$ Heisenberg antiferromagnets with nearest-neighbor exchange on the highly frustrated pyrochlore lattice.^{6,11,12} The size of the nonmagnetic ion determines the Cr-Cr distance and thereby the strength of exchange: 4.5 meV for Zn,⁶ 1 meV for Cd,¹¹ and a fraction of a meV for Hg.¹²

CdCr₂O₄ undergoes a spin-Peierls-like lattice distortion^{4,5} at $T_c=7.8$ K.¹¹ The lattice symmetry is lowered from cubic ($Fd\bar{3}m$) to tetragonal (exact space group unknown) with lattice constants $a=b \neq c$. The unit cell is elongated: $(c-a)/c \approx 5 \times 10^{-3}$. In contrast, the lattice is flattened, $(c-a)/c \approx -1.5 \times 10^{-3}$, in ZnCr₂O₄. It is remarkable that distortions in two very similar compounds have opposite signs. It is also surprising that the magnitude of the distortion is larger in the compound with weaker magnetic interactions. This happens, apparently, because the quantity $(c-a)/c$ measures the uniform part of the distortion only. There are indications^{6,7} that the nonuniform distortions in ZnCr₂O₄ are much larger than the uniform component. We will work under the assumption that the lattice distortion in CdCr₂O₄ low-

ers the point-group symmetry of the lattice but leaves the translational symmetry intact.¹⁰

The spins in CdCr₂O₄ remain disordered well below the Curie-Weiss temperature and order simultaneously with the distortion. Chung *et al.*¹¹ interpret the magnetic order as an incommensurate spiral with the wave vector $\mathbf{q}=2\pi(0, \delta, 1)$ and the magnetization in the *ac* plane. They offer two ordered structures compatible with the magnetic Bragg peaks. In one the spins on every tetrahedron are nearly orthogonal (say, close to directions $+\hat{x}$, $+\hat{z}$, $-\hat{x}$, and $-\hat{z}$ on some tetrahedra), in the other they are nearly collinear (say, two along $+\hat{x}$ and two along $-\hat{x}$). Since $\delta \approx 0.09$ is small, we may treat it as an effect of a weak perturbation and begin our analysis at the commensurate point $\delta=0$.

The Landau theory of a deformable pyrochlore antiferromagnet¹⁰ yields a variety of magnetically ordered states, with the proposed orthogonal and collinear states among them. Thus, from the symmetry viewpoint, both candidate orders are plausible. However, a more “microscopic” treatment based on the actual physics of the spin-lattice coupling (and as we will see, first-principles total energy calculations) invariably yields collinear ground states. Stabilization of orthogonal ground states requires fairly exotic interactions, such as a four-spin exchange *strongly* coupled to the lattice.¹⁰ We therefore abandon the orthogonal state and work with the collinear one.

To simplify the calculations, we assume a clear separation of relevant energy scales. We treat the nearest-neighbor Heisenberg exchange as the strongest interaction; its minimization requires that the total spin of every tetrahedron be zero, which still leaves a high-dimensional continuum of ground states.² A weaker spin-lattice coupling selects from this continuum a collinear ground state. The weakest Dzyaloshinskii-Moriya (DM) interaction induces a slight misalignment of the spins and—in the presence of parity breaking—generates a spiral with a long period. In this paper we outline our findings, postponing a detailed account to a future presentation.¹³

In a flexible pyrochlore antiferromagnet, the spin-lattice coupling is an efficient way to relieve spin frustration.^{4,5} The magnetoelastic coupling arises from the dependence of exchange on the ion displacements x_α of spins: E_{me}

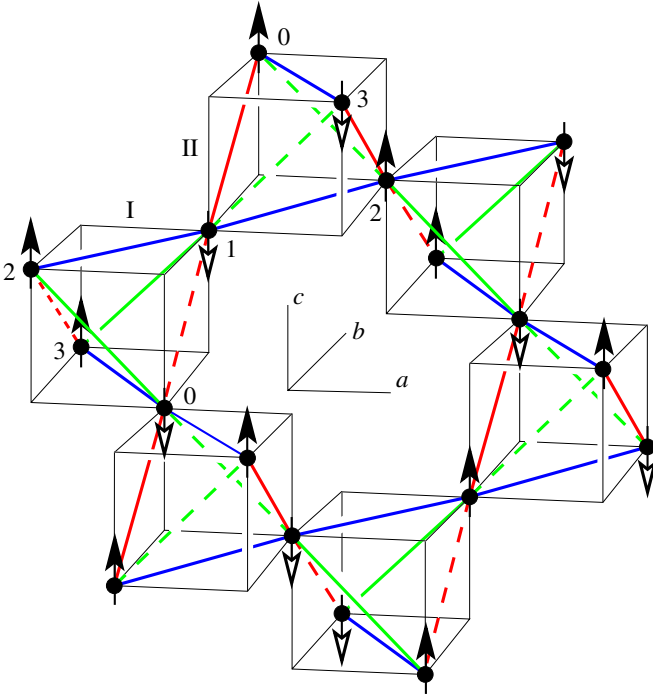


FIG. 1. (Color online) The collinear ground state stabilized by the $\mathbf{q}=\mathbf{0}$ E_u phonon (adapted from Fig. 6 of Ref. 10). Tetrahedra of types I and II are flattened along the a and b directions, respectively. Solid (dashed) lines indicate satisfied (frustrated) bonds. Frustrated bonds form spirals of the same handedness (left handed in this case).

$=(\partial J_{ij}/\partial x_\alpha)(\mathbf{S}_i \cdot \mathbf{S}_j)x_\alpha$. Integrating out the phonons generates an effective biquadratic exchange $-\sum_{i,j}(\mathbf{S}_i \cdot \mathbf{S}_j)^2$ favoring collinear ground states. Alternatively, this interaction can be written in terms of the magnetoelastic force $\mathbf{f}=(f_1, f_2)$ whose components are linear combinations of the bond variables $\mathbf{S}_i \cdot \mathbf{S}_j$ transforming as an irreducible doublet E of the tetrahedral group T_d .¹⁰ For a single tetrahedron, the magnetoelastic energy is $-J'^2|\mathbf{f}|^2/2k$, where J' is a derivative of the exchange with respect to ionic coordinates and k is the elastic constant of the vibrational doublet E . The energy is lowest in a state with a tetragonal distortion, two weak and four strong bonds, and collinear spins.⁵

When a distortion preserves the translational symmetry of the crystal, generalization to an infinite lattice is straightforward.¹⁰ The existence of inequivalent tetrahedra with two different orientations (I and II in Fig. 1) adds inversion to the symmetry group enlarging it to $T_d \otimes I = O_h$. The magnetoelastic energy of a primitive unit cell (four Cr ions) is

$$E_{me} = -K_g|\mathbf{g}|^2/4 - K_u|\mathbf{u}|^2/4, \quad (1)$$

where $\mathbf{g}=\mathbf{f}^I+\mathbf{f}^{II}$ and $\mathbf{u}=\mathbf{f}^I-\mathbf{f}^{II}$ are the even and odd doublets of bond variables whose coupling constants are $K_{g,u}=J'^2/k_{g,u}$, where k_g and k_u are the elastic constants of the even and odd distortion doublets. For $K_g > K_u$ the lattice undergoes a uniform tetragonal distortion with $a=b > c$; the space group is $I4_1/amd$. For $K_g < K_u$ the distortion has both even and odd components: tetrahedra of types I and II are

flattened along the a and b directions, respectively; the lattice is elongated overall, $a=b < c$; the space group $I4_122$ lacks inversion symmetry. In both cases the ground states are collinear (Figs. 5 and 6 of Ref. 10).

The antiferromagnetic order on the pyrochlore lattice can be described by three staggered magnetizations \mathbf{L}_i defined on tetrahedra of type I: $\mathbf{L}_1=(\mathbf{S}_0+\mathbf{S}_1-\mathbf{S}_2-\mathbf{S}_3)/4S$, and so on. The vanishing of the total spin of a tetrahedron in a ground state $\mathbf{M}^I=\sum_{i=0}^3\mathbf{S}_i=\mathbf{0}$ makes the three Néel vectors \mathbf{L}_i orthogonal to each other and imposes a constraint on their lengths: $\sum_{i=1}^3L_i^2=1$. In the state shown in Fig. 1, $\mathbf{L}_2=\mathbf{L}_3=\mathbf{0}$ and $\mathbf{L}_1=\hat{\mathbf{n}}_1e^{i\mathbf{q}\cdot\mathbf{r}}$ with $\mathbf{q}=2\pi(0,0,1)$; $\hat{\mathbf{n}}_1$ is an arbitrary unit vector. This is also consistent with the data¹¹ if we take the commensurate limit $\delta \rightarrow 0$.

Spiral magnetic order can arise when competing interactions destabilize a collinear ground state. That can happen when, e.g., the second-neighbor exchange is comparable to the nearest-neighbor one. However, further-neighbor exchanges are rather weak in spinels ACr_2O_4 and we have checked that they do not destabilize collinear order (see below).

Alternatively, spiral magnetic order may reflect a chiral nature of the underlying lattice. The handedness is transferred from the lattice to the spins by the relativistic spin-orbit coupling $\alpha(\mathbf{L} \cdot \mathbf{S})$. Cubic spinels are nonchiral: the space group $Fd\bar{3}m$ includes inversion. However, parity is broken in the presence of the odd distortion E_u . A chiral nature of the distorted lattice becomes evident if one examines the locations of frustrated bonds shown as dashed lines in Fig. 1: they form spirals of the same handedness. Since the symmetry breaking is spontaneous, experiments should reveal both right- and left-handed magnetic spirals originating in different domains.

In a Heisenberg magnet the spin-orbit interaction is manifested as the DM term $\mathbf{D}_{ij} \cdot [\mathbf{S}_i \times \mathbf{S}_j]$.¹⁴ Elhajal *et al.*¹⁵ have determined the vectors \mathbf{D}_{ij} for the pyrochlore lattice up to a multiplicative constant. In a single tetrahedron, the DM term is

$$E_{DM} = -DS^2(\hat{\mathbf{a}} \cdot \mathbf{L}_2 \times \mathbf{L}_3 + \hat{\mathbf{b}} \cdot \mathbf{L}_3 \times \mathbf{L}_1 + \hat{\mathbf{c}} \cdot \mathbf{L}_1 \times \mathbf{L}_2). \quad (2)$$

Using the commensurate state as a starting point we parametrize the magnetic structure as

$$\mathbf{L}_i(\mathbf{r}) = e^{i\mathbf{q}\cdot\mathbf{r}}\phi_i(\mathbf{r})\hat{\mathbf{n}}_i(\mathbf{r}), \quad (3)$$

where $\hat{\mathbf{n}}_i(\mathbf{r})$ and $\phi_i(\mathbf{r})$ are the directions and magnitudes of the staggered magnetizations. [Note that the three unit vectors $\hat{\mathbf{n}}_i(\mathbf{r})$ are mutually orthogonal.] These parameters vary slowly in space. Proximity to the collinear state means that ϕ_2 and ϕ_3 are small, while $\phi_1 \approx 1 - (\phi_2^2 + \phi_3^2)/2$. The staggered magnetizations (3) are defined for tetrahedra of type I. Tetrahedra of type II become slaves: their magnetic state is encoded in the staggered magnetizations of the four surrounding tetrahedra of type I. The vanishing of the total magnetization of type-II tetrahedra yields the following constraint:

$$\mathbf{M}^{\text{II}} = \phi_3 \hat{\mathbf{n}}_3 - \partial_y \hat{\mathbf{n}}_1 / 4 = \mathbf{0}. \quad (4)$$

From it we infer that spatial derivatives of $\hat{\mathbf{n}}_1$ are of the same order as ϕ_2 and ϕ_3 . The Néel magnetizations of a type-II tetrahedron are, to lowest orders,

$$\mathbf{L}_1^{\text{II}} = \phi_2 \hat{\mathbf{n}}_2 - \partial_z \hat{\mathbf{n}}_1 / 4, \quad \mathbf{L}_2^{\text{II}} = \hat{\mathbf{n}}_1, \quad \mathbf{L}_3^{\text{II}} = -\partial_x \hat{\mathbf{n}}_1 / 4. \quad (5)$$

Upon adding contributions from tetrahedra of both types and using Eq. (4) we obtain the DM energy

$$E_{\text{DM}} = -DS^2 \hat{\mathbf{n}}_1 \cdot (\hat{\mathbf{a}} \times \partial_x \hat{\mathbf{n}}_1 + \hat{\mathbf{b}} \times \partial_y \hat{\mathbf{n}}_1 - \hat{\mathbf{c}} \times \partial_z \hat{\mathbf{n}}_1) / 4. \quad (6)$$

The terms linear in the spatial derivatives make a uniform state unstable against the formation of a spiral.¹⁶ The pitch of the spiral depends on the stiffness of the staggered magnetization, which is ordinarily determined by the strength of exchange. However, the large degeneracy of the pyrochlore antiferromagnet with nearest-neighbor exchange leads to a vanishing stiffness: indeed, apart from the constraint (4), the direction of $\hat{\mathbf{n}}_1$ can vary arbitrarily in space. The stiffness is therefore determined by the magnetoelastic coupling and by weak exchange interactions beyond nearest neighbors. We discuss the magnetoelastic coupling first.

A spiral magnetic state represents a deviation from the collinear structure and thus increases the magnetoelastic energy. On symmetry grounds, the increase should be quadratic in the gradients of $\hat{\mathbf{n}}_1$ and thus may yield a finite stiffness. For simplicity, we first consider only the odd distortions, effectively setting $k_g = \infty$ and $K_g = 0$ in Eq. (1), and discuss the influence of the even phonon later. The magnetoelastic energy can then be expressed in terms of the odd doublet as $E_{\text{me}} = -K_u \mathbf{u} \cdot \delta \mathbf{u} / 2$, where $\mathbf{u} = 4S^2(0, 1)$ is the value in the commensurate ground state and $\delta \mathbf{u}$ is a small deviation. As a result, we obtain the magnetoelastic energy density as a function of ϕ_i and the gradients of $\hat{\mathbf{n}}_i$. However, on account of the constraint (4), $\phi_3 = \hat{\mathbf{n}}_3 \cdot \partial_y \hat{\mathbf{n}}_1 / 4$. Likewise, minimization of the energy with respect to ϕ_2 yields

$$\phi_2 = \hat{\mathbf{n}}_2 \cdot \partial_z \hat{\mathbf{n}}_1 / 8. \quad (7)$$

The energy cost associated with the spiral is then

$$E_{\text{me}} = K_u (S^4 / 4) [(\partial_x \hat{\mathbf{n}}_1)^2 + (\partial_y \hat{\mathbf{n}}_1)^2 + 2(\partial_z \hat{\mathbf{n}}_1)^2 - (\hat{\mathbf{n}}_2 \cdot \partial_z \hat{\mathbf{n}}_1)^2]. \quad (8)$$

The total energy of a spiral state is the sum of the DM energy (6) and the magnetoelastic energy (8). Its minimization yields three simple spiral states in which $\hat{\mathbf{n}}_1$ rotates about one of the principal axes staying in the plane perpendicular to it, e.g., $\hat{\mathbf{n}}_1 = (0, \cos(\theta(x)), \sin(\theta(x)))$. The energy density of all three states is the same,

$$E = -DS^2 \theta' + K_u S^4 \theta'^2 / 4, \quad (9)$$

where, in this case, $\theta' = \partial_x \theta$. The pitch of the spiral is

$$\theta' = 2\pi\delta = 2D/S^2 K_u. \quad (10)$$

A spiral state with spins rotating about the a axis is shown in Fig. 2(a). On account of Eqs. (4) and (7), we have $\phi_2 = \phi_3 = 0$, so that type-I tetrahedra still have collinear spins.

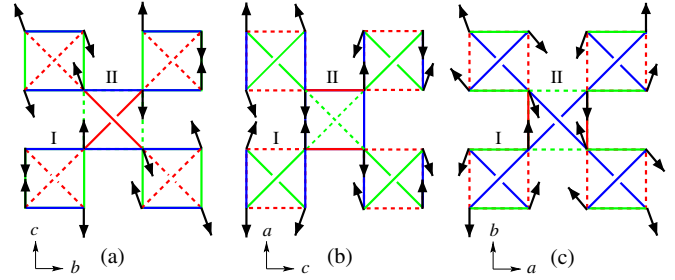


FIG. 2. (Color online) Spiral magnetic orders with the spins rotating about (a) the a , (b) the b , and (c) the c axis.

The spins on type-II tetrahedra are coplanar with the twist angle of $\theta' / 4 = \pi\delta / 2$. The spiral magnetic order produces Bragg scattering at $\mathbf{q} = 2\pi(-\delta, 0, 1)$.

Figure 2(b) shows a spiral state twisting about the b axis. This time tetrahedra of type I have coplanar spins with the twist angle $\phi_3 = \theta' / 4 = \pi\delta / 2$, while tetrahedra of type II have collinear spins, as can be checked by using Eq. (5). This spiral is related to the previous one by a lattice symmetry (the inversion and a $\pi/2$ rotation in the xy plane). It produces a magnetic Bragg peak at $\mathbf{q} = 2\pi(0, \delta, 1)$, as observed by Chung *et al.*¹¹ The measured value¹¹ $\delta \approx 0.09$ is consistent with a DM interaction that is weak relative to the magnetoelastic coupling: $D/K_u S^2 \approx 0.28$.

The third spiral solution is shown in Fig. 2(c). It has the wave vector $\mathbf{q} = 2\pi(0, 0, 1 + \delta)$; the spins are rotating around the c axis. The twist angle is $\phi_2 = \delta\pi / 4$.

The degeneracy of the three spiral ground states is lifted when other perturbations are taken into account. A uniform E_g distortion and the further-neighbor exchanges J_2 and J_3 add energy terms

$$K_g (S^4 / 4) [(\partial_x \hat{\mathbf{n}}_1)^2 + (\partial_y \hat{\mathbf{n}}_1)^2] + (4J_3 - 2J_2) S^2 (\partial_z \hat{\mathbf{n}}_1)^2. \quad (11)$$

Depending on these coupling constants, the system will prefer the spiral states shown either in Figs. 2(a) and 2(b) or in Fig. 2(c).

To test this theory, we performed density-functional calculations within the local spin density approximation LSDA+ U method¹⁷ using projector augmented-wave potentials as implemented in the Vienna *ab initio* Simulation Package.^{18,19} Values for the on-site Coulomb and exchange parameters, $U = 3$ eV and $J = 0.9$ eV, were chosen as previously described.²⁰ The results are not particularly sensitive to reasonable variations of U (± 1 eV). First we performed full structural relaxations in the 14-atom cubic unit cell, space group $Fd\bar{3}m$. Chromium ions were initialized with parallel spins in order to retain O_h symmetry throughout the structural relaxation. The relaxed lattice constant $a = 8.54$ Å was found to be in excellent agreement with $a = 8.59$ Å measured by Chung *et al.*¹¹

Estimates of exchange constants were obtained by comparing the total energy for several simple spin configurations. To prevent contamination by magnetoelastic terms (1), the lattice structure was frozen in the reference cubic state with $a = 8.54$ Å. That procedure yielded $J_1 = 0.5$ meV, J_2

≈ 0 meV, and $J_3=0.15$ meV. The resulting Curie-Weiss temperature $\Theta_{\text{CW}}=-(1/3k_B)S(S+1)\sum_i z_i J_i=-70$ K compares well to the experimental values ranging from -70 to -90 K.^{8,11}

To quantify the magnetoelastic effects, we performed full structural relaxations for three spin configurations: (i) a collinear state with a pure E_g distortion and magnetic wave vector $\mathbf{q}=\mathbf{0}$ shown in Fig. 5 of Ref. 10; (ii) a coplanar state with a pure E_g distortion and $\mathbf{q}=2\pi(0,0,1)$; and (iii) a collinear state with a mixed E_u+E_g distortion and $\mathbf{q}=2\pi(0,0,1)$ shown in Fig. 1. States (ii) and (iii) are the commensurate limits ($\delta\rightarrow 0$) of the states displayed in Figs. 3(c) and 3(d) of Ref. 11; they have a doubled unit cell (28 atoms). The total energy was lowest in the collinear state (iii), as posited above. The E_g component of the distortion is tetragonal. Its value, $(c-a)/c=+5.1\times 10^{-3}$, is remarkably close to the experimental one.¹¹ Reduction of the energy associated with the structural relaxation depends on the spin state according to Eq. (1). From the data obtained in the three reference states we deduced the magnetoelastic constants $K_u=0.15$ meV $>$ $K_g=0.13$ meV. Quantitatively, the spin-lattice coupling is weaker than exchange, although not by much: $K_u S^2/J_1=0.67$.

The *ab initio* calculations back up the conclusions obtained analytically. The phonon doublet E_u indeed turned out to be softer than the even distortion E_g confirming the selection of the collinear state of Fig. 1. The competition between the three candidate spiral states is decided by the ratio of the coupling constants in Eq. (11). Because J_3 is quite large, the last term is prohibitively expensive and the spiral twists along either x or y , as indeed observed.¹¹

A large value of J_3 may cast doubts on the applicability of Eq. (11), which treats that coupling as a small perturbation. However, it turns out that our conclusions in that regard remain valid for arbitrarily large values of J_3 . Luckily for us, the spiral states depicted in Figs. 2(a) and 2(b) minimize the third-neighbor exchange exactly for any value of the pitch δ .¹³ The third spiral state increases the J_3 term and is thus suppressed.

To appreciate the unusual microscopic origin of the magnetic spiral, it is helpful to compare it to the standard scenario exemplified by the ferroelectric BiFeO₃.²¹ In the latter case, the pitch of the magnetic spiral is proportional to an order parameter measuring the violation of parity, such as the electric dipolar moment. In contrast, in CdCr₂O₄ the strongest violation of parity comes not so much from the lattice distortion as from the magnetically ordered state itself: frustrated bonds form spirals of the same handedness (Fig. 1). The corresponding order parameter¹⁰ the odd doublet of bond variables \mathbf{u} —is a dimensionless quantity of order 1, which is why the presence of an order parameter is not immediately evident in Eq. (10). Without parity violation, the DM interaction alone would not generate a magnetic helix.

Note added in proof. The three staggered magnetizations were first introduced in Ref. 22.

We thank C. Broholm, D. Clarke, H. D. Drew, C. L. Henley, S.-H. Lee, R. Moessner, and A. B. Sushkov for stimulating discussions. This work was supported in part by the NSF Grant No. DMR-0348679.

¹R. Moessner and A. P. Ramirez, Phys. Today **59**(2), 24 (2006).

²R. Moessner and J. T. Chalker, Phys. Rev. B **54**, 5006 (1996).

³A. P. Ramirez, A. Hayashi, R. J. Cava, R. Siddharthan, and B. S. Shastry, Nature (London) **399**, 333 (1999).

⁴Y. Yamashita and K. Ueda, Phys. Rev. Lett. **85**, 4960 (2000).

⁵O. Tchernyshyov, R. Moessner, and S. L. Sondhi, Phys. Rev. Lett. **88**, 067203 (2002).

⁶S. H. Lee, C. Broholm, T. H. Kim, W. Ratcliff II, and S.-W. Cheong, Phys. Rev. Lett. **84**, 3718 (2000).

⁷A. B. Sushkov, O. Tchernyshyov, W. Ratcliff II, S. W. Cheong, and H. D. Drew, Phys. Rev. Lett. **94**, 137202 (2005).

⁸H. Ueda, H. A. Katori, H. Mitamura, T. Goto, and H. Takagi, Phys. Rev. Lett. **94**, 047202 (2005).

⁹C. Broholm (private communication).

¹⁰O. Tchernyshyov, R. Moessner, and S. L. Sondhi, Phys. Rev. B **66**, 064403 (2002).

¹¹J.-H. Chung, M. Matsuda, S.-H. Lee, K. Kakurai, H. Ueda, T. J. Sato, H. Takagi, K.-P. Hong, and S. Park, Phys. Rev. Lett. **95**, 247204 (2005).

¹²H. Ueda, H. Mitamura, T. Goto, and Y. Ueda, Phys. Rev. B **73**, 094415 (2006).

¹³G.-W. Chern *et al.* (unpublished).

¹⁴T. Moriya, Phys. Rev. **120**, 91 (1960).

¹⁵M. Elhajal, B. Canals, R. Sunyer, and C. Lacroix, Phys. Rev. B **71**, 094420 (2005).

¹⁶I. E. Dzyaloshinskii, Sov. Phys. JETP **19**, 960 (1964).

¹⁷V. I. Anisimov, F. Aryasetiawan, and A. I. Lichtenstein, J. Phys.: Condens. Matter **9**, 767 (1997).

¹⁸G. Kresse and J. Hafner, Phys. Rev. B **47**, R558 (1993); G. Kresse and J. Furthmüller, *ibid.* **54**, 11169 (1996).

¹⁹P. E. Blöchl, Phys. Rev. B **50**, 17953 (1994); G. Kresse and D. Joubert, *ibid.* **59**, 1758 (1999).

²⁰C. J. Fennie and K. M. Rabe, Phys. Rev. Lett. **96**, 205505 (2006); Phys. Rev. B **72**, 214123 (2005).

²¹A. M. Kadomtseva, A. K. Zvezdin, Yu. F. Popov, A. P. Pyatakov, and G. P. Vorob'ev, JETP Lett. **79**, 571 (2004).

²²C. L. Henley and N.-g. Zhang, Phys. Rev. Lett. **81**, 5221 (1998).